Is diffusion weighted imaging adding value in diagnosis of focal hepatic lesions? Experience in 50 patients

CrossMark

Doaa Mokhtar Mohamed Emara [a,*], **Fouad Serag El-Din Mohamed** [a], **Ahmed Hamimi Abdullah** [a], **Mona Abdel-Hadi Ibrahim** [b], **Mohamed Eid Ibrahim** [a], **Ehab Mostafa Hassouna** [c]

[a] Radiology Department, Alexandria University, Faculty of Medicine, Eygpt
[b] Pathology Department, Alexandria University, Faculty of Medicine, Eygpt
[c] Internal Medicine Department, Alexandria University, Faculty of Medicine, Eygpt

Abstract *Introduction:* Diffusion weighted imaging (DWI) offers molecular information that complements the morphologic information obtained with conventional magnetic resonance imaging (MRI) and can reflect the functions and structures of the body without trauma.

Aim of the work: To assess the role of DWI as a routine sequence in a MRI study to help in differentiating liver lesions.

Patients and methods: The study included 50 patients referred to do a MRI study to diagnose and/or to confirm the ultrasonographic or CT findings of focal hepatic lesions. The examination was done on 1.5T superconducting magnet MRI machines; Philips Gyroscan Intera version 12.1.1.2 (Best, The Netherlands) and Siemens Magnetom Avanto (Erlangen, Germany) machine.

Results: All studied patients had a focal hepatic lesion either on top of cirrhotic liver or non cirrhotic liver. DWI was found to be helpful with the routine MRI sequences to reach the diagnosis. The final diagnosis was confirmed by histopathological examination or follow up.

A cutoff value of ADC for benign lesions was found to be 1.25×10^{-3} mm^2/s.

Conclusions: DWI should be included as a basic sequence in the routine MRI study of the liver as it helps in diagnosis and so reaching a final diagnosis or at least trying to narrow the list of differential diagnosis.

© 2013 Alexandria University Faculty of Medicine. Production and hosting by Elsevier B.V. All rights reserved.

1. Introduction

MRI plays an increasingly important role in the evaluation of patients with liver disease because of its high contrast resolution, lack of ionizing radiation, and the possibility of performing functional imaging sequences. With advances in hardware and coil systems, diffusion weighted imaging (DWI) can now be applied to liver imaging with improved image quality.[1,2]

DWI offers molecular information that complements the morphologic information obtained with conventional MRI, and can reflect the functions and structures of the body without trauma and as an index for assessing the tumor response to treatment.[3–6]

1.1. Principles of DW MRI

DWI exploits the random motion of water molecules. In a totally unrestricted environment, water movement would be completely random, a phenomenon otherwise known as Brownian motion or free diffusion.[7]

Within biologic tissues, the movement of water is not completely random, but rather, is impeded by the interaction with tissue compartments, cell membranes, and intracellular organelles. For purposes of simplification, water movement in tissues may be categorized as intravascular, intracellular, or extracellular (Fig. 1).[1,8]

The extent of tissue cellularity and the presence of intact cell membranes help determine the impedance of water molecule diffusion. Tissue types that have been reported to be associated with impeded diffusion include tumor, cytotoxic edema, abscess, and fibrosis. Tissues with low cellularity or that
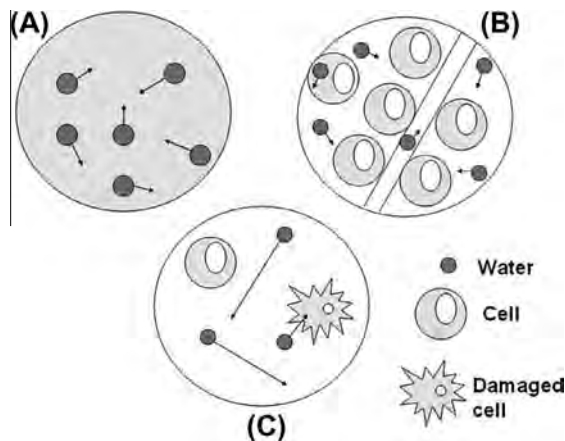
Figure 1 Schematic illustrating water molecule movement. In (A) water molecules in a container alone move randomly (Brownian motion). In (B) highly cellular tissue impedes the movement of water molecules. Their movement can be categorized as intravascular, intracellular, or extracellular. In (C) tissue of low cellularity or with defective cells permits greater water molecule movement.[1]

consist of cells with disrupted membranes permit greater movement of water molecules.[6]

The spin-echo T2-weighted sequence consists of a 90° radiofrequency (RF) pulse followed by a 180° RF pulse, with the T2 decay related to transverse relaxation. Measurement of water diffusion is possible with the application of a dephasing gradient (diffusion sensitizing gradient) prior to the 180° RF pulse. A symmetric rephasing gradient is then applied after the 180° RF pulse (Fig. 2a). In a simplified model, the effect of the first (dephasing) gradient is cancelled out by the second (rephasing) gradient in tissues with limited or impeded water movement, such as the highly cellular tissue of tumors. Therefore, there is little impact on the overall T2 decay, and the T2 signal of the tissue is maintained. In tissues with unimpeded water movement (low cellularity tissue), water molecules may move a considerable distance between the dephasing and rephasing gradient applications. Consequently, the mobile water molecules will not be fully rephased, resulting in a reduction in overall T2 signal intensity (Fig. 2b).[1,6]

1.2. Choice of b values and sequence optimization

Because of the relatively short T2 relaxation time of the normal liver parenchyma, the b values used for clinical imaging are typically no higher than 1000 s/mm². Applying a small diffusion weighting of b less than 100–150 s/mm² nulls the intrahepatic vascular signal, creating the so-called black-blood images, which improve the detection of focal liver lesions (Fig. 3) while higher b values ($\geqslant 500$ s/mm²) give diffusion information that helps in focal liver lesion characterization. Hence, when performing DW MR imaging in the liver, it is advantageous to perform imaging by using both lower and higher b values (e.g., $b \geqslant 50$, $b \geqslant 100$, and $b \geqslant 500$ s/mm²).[9–12]

1.3. Qualitative visual assessment

Visual assessment is helpful for disease detection and characterization by observing the differential signal attenuation between tissues on DW MRI. Cellular tissues will demonstrate restricted diffusion (high signal intensity) and lower ADC values.[1]

1.4. Quantitative analysis of DWI findings and ADC

The ADC represents the slope (gradient) of a line that is produced when the logarithm of relative signal intensity of tissue is plotted along the y-axis versus b values along the x-axis thereby linearizing the exponential decay function. Quantitative analysis of diffusion-weighted imaging findings can be performed only if at least two b values are used for imaging.[13–15]

The analysis of ADC is an automated process that is available as an application on most scanners or on a workstation. The ADC can then be displayed as a parametric map and essentially reflects differences in tissue diffusivity at different b values. ADC measurements are then recorded
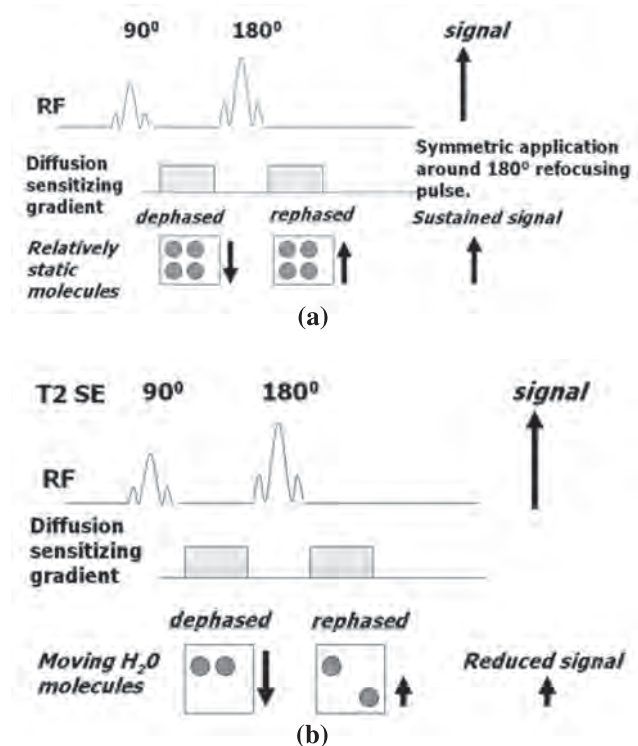
Figure 2 (a) Schematic illustrating the effect of a diffusion-weighted sequence on water molecules (solid circles) within highly cellular tissue or a restricted environment. The diffusion-weighted sequence is fundamentally a T2-weighted sequence with the application of a dephasing gradient (diffusion sensitizing gradient) prior to the 180° RF pulse, followed by a symmetric rephasing gradient after the 180° pulse. Water molecules within a restricted environment do not move long distances and acquire phase shifts during the application of the first gradient that are cancelled out by phase shifts acquired during the second (opposing) gradient. As a result, no net loss in signal intensity occurs (aside from normal T2 decay).[1] (b) Schematic illustrating the effect of a diffusion-weighted sequence on water molecules (solid circles) within tissue with low cellularity or a less restricted environment. Water molecules within a less restricted environment can move long distances. Such highly mobile molecules acquire phase information from the first gradient, but because of their motion, their signal does not completely rephase with the second gradient, resulting in a net loss in signal intensity in addition to normal T2 decay SE = spin-echo.[1]

for a given region by drawing regions of interest on the ADC map.[1,6]

However, the signal intensity observed on the diffusion image is dependent on both the water proton diffusivity and the tissue T2-relaxation time, which is a possible confounding factor. This means that a lesion may appear to show restricted diffusion on DW MR Images because of the long T2-relaxation time rather than the limited mobility of the water protons (T2 shine-through). This phenomenon can be observed in the normal gallbladder, cystic lesions, and hemangiomas. The presence of T2 shine-through is recognized by correlating high-*b*-value images with the ADC map. Areas demonstrating substantial T2 shine-through rather than restricted diffusion

will show high diffusivity on the ADC map and high ADC values (Figs. 4 and 5).[2]

Areas of true restricted diffusion demonstrate high signal intensity on diffusion-weighted images with corresponding low signal intensity on the ADC map; areas of relatively free diffusion also appear bright on diffusion-weighted images, corresponding to T2 shine-through effects, but will also stay bright on the ADC map.[6]

2. Methods

2.1. Study population

The study population included 50 patients referred to do MRI study to diagnose and/or to confirm the ultrasonographic or CT findings of focal hepatic lesions.

2.2. Imaging technique

All patients had ultrasound as a routine examination (showing the lesions), CT was done to diagnose these lesions and to confirm or further characterize the CT findings, MRI was done.

Ultrasound examination was done for all patients to show whether the liver is cirrhotic or not, to diagnose the presence of the hepatic lesion and if there is any other abnormalities in the abdomen, e.g., enlarged LN, ascites other lesions in the spleen, kidney or pancreas.

Triphasic CT of the liver was done for all patients who helped in the diagnosis of hypervascular lesions as HCC, focal nodular hyperplasia (FNH) which was evident in the hepatic arterial phase (HAP) and other lesions such as metastases which were evident in the portal venous phase (PVP) and the delayed phase. Hemangiomas and focal confluent fibrosis were evident by their enhancement dynamics in the three phases mainly delayed filling in.

2.3. MRI imaging

All patients in this study were imaged using 1.5T superconducting magnet MRI machines; Philips Gyroscan Intera version 12.1.1.2 (Best, The Netherlands) and Siemens Magnetom Avanto (Erlangen, Germany).

Pre scanning fasting was done for at least 4 h and patients were instructed about the examination and its time, and how to take and keep a deep breath which is required in certain sequences e.g., triphasic study after contrast injection.

The patient was placed in the supine position; arms extended above the head. A phased array surface coil was used. Respiratory-gated acquisitions were used in some sequences. Typical scan time was 20–30 min.

2.4. Scanning parameters

○ Localizing T1-W gradient echo sequences were used.
○ Axial 2D T2-W turbo spin echo (HASTE/TSE) fat suppression sequence from the level of lower chest to the mid abdomen level as finishing the whole liver span. TR1600, TE 70, flip angle 90, FOV 375, slice thickness 7 mm., NSA 1 total scan time averaging 43 s.
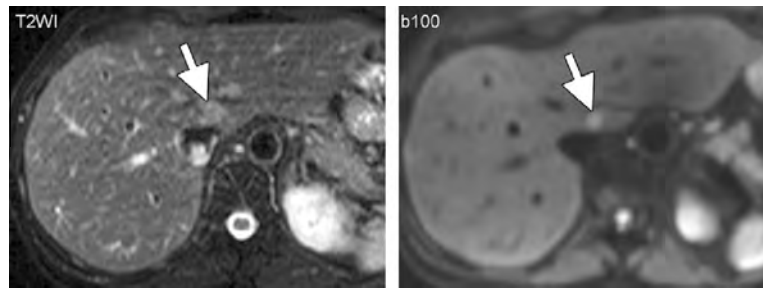
Figure 3 Lesion detection with DW MR imaging versus T2-weighted imaging. Transverse fat-suppressed (left) turbo SE T2-weighted image and (right) single-shot SE echo-planar diffusion image ($b \, 5 \times 100$ s/mm^2) in a 54-year-old man with colorectal cancer. Application of diffusion weighting with small b value eliminates the high signal intensity from the intrahepatic vasculature, which makes the metastasis (arrows) in the caudate lobe of the liver more conspicuous on DW MR image than on T2-weighted image.[1,13]

○ Axial 2D T2-W turbo spin echo (HASTE/TSE) fat suppression sequence with longer TE = 190.

○ In-phase and opposed phase (IP/OP) sequence. TR 500, TE 4.6, FOV 375, flip angle 80, slice thickness 7 mm, NSA 2, average scanning time 48 s.

○ SSFP (BFFE in Philips). TR 500, TE 60, flip angle 60, FOV 255, slice thickness 7 mm, NSA 1 with average scan time of 22 s.

○ DWI with variable b values 50–1000 s/mm^2 with TR 1000, TE 137, flip angle 90, FOV 370, slice thickness 10 mm and average scan time 1.15 min.

○ 3D T1 spoiled gradient fat suppression sequence (THRIVE in Philips and VIBE in Siemens) with TR 50,TE 500, FOV 355, flip angle 10, slice thickness 3 mm with average scan time 19 s and this is repeated in the triphasic study as HAP (15 s after the end of contrast injection), PVP (70 s from the end of contrast injection) and delayed phase (about 3 min from the end of contrast injection) and this delayed phase may be repeated if indicated in certain cases e.g., with fibrous components as cholangiocarcinoma or metastasis with fibrous tissues

2.5. Post processing and interpretation

The source images were transferred to a dedicated workstation for post-processing. The two dimensional series served to provide detailed anatomical data and reference scans. DWI was interpreted in correlation with ADC amp and ADC value was calculated in 10^{-3} mm^2/s. Multiplanner reconstruction (MPR) was used to interpret T1 spoiled gradient sequence in 3D triphasic study (pre and post contrast phases). All sequences were interpreted and finally we reached the diagnosis which was confirmed by histopathological findings in indicated cases or by follow up.

3. Results

Out of the 50 patients included in this study 34 were males and 16 were females.

The age of the studied patient ranged from 25 to 78 years with a mean age of 53.5 years Fig. 6.

The distribution of focal hepatic lesions was as follows in the pie chart (Fig. 7).

Description of imaging findings and their correlation with pathology and or follow up:

One patient had a dysplastic nodule which was large in size and showed no diffusion restriction. This patient was diagnosed by CT as HCC while MRI showed the classic signal intensity of the dysplastic nodules (T2 hypointense, T1 hyperintense) with no diffusion restriction, enhancement in HAP with gradual fading in PVP and delayed phase (Fig. 8). Histopathological examination confirmed the MRI diagnosis of dysplastic nodule.

Three patients had focal confluent fibrosis with characteristic delayed enhancement and no diffusion restriction with ADC ranging from 1.4 to 1.6×10^{-3} mm^2/s (Fig. 9). Patients with focal confluent fibrosis showed the lesions in CT but to confirm this diagnosis, especially in patients with cirrhotic livers and suspicion of HCC, MRI was done. This latter showed the characteristic signal intensity of the lesions with no diffusion restriction as well as delayed enhancement and also excluded the presence of HCC.

One patient had post TACE scar showing minor foci of activity that shows diffusion restriction and ADC = 1×10^{-3} mm^2/s. In this patient the CT showed no activity while MRI showed minor activity.

Twenty patients had HCC on top of cirrhotic livers showing the typical findings of HCC with diffusion restriction and ADC value ranging from 0.7 to 1.1×10^{-3} mm^2/s (Fig. 10).

In patients with HCC the two dynamic studies (triphasic CT and MRI) were enough for diagnosis of HCC with no need for further histopathological evaluation.

One HCC case showed portal vein malignant thrombus that showed the same enhancement dynamics, diffusion restriction and ADC value of the main (HCC) lesion (Fig. 11).

Five patients had metastases from different primaries. Some of these metastases showed delayed enhancement reflecting the presence of fibrous components, and there was diffusion restriction of these lesions of ADC ranging from 0.8 to 1.4×10^{-3} mm^2/s (Fig. 12).

In patients with metastases we relied on the history of primary tumor and the presence of multiple hepatic lesions on top of non cirrhotic liver to confirm the diagnosis. All cases with metastases on follow up showed either stationary or regressive course of the disease.
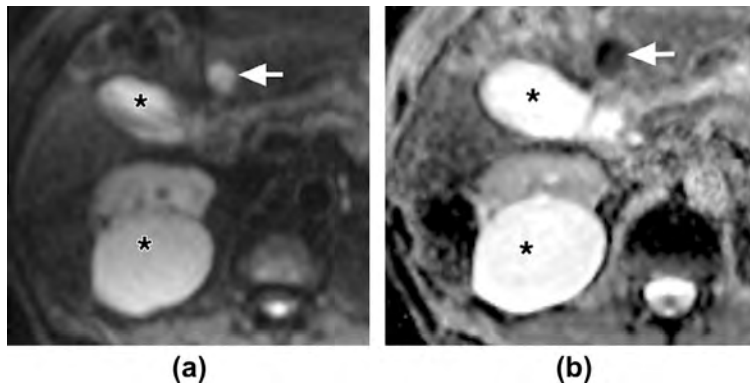
Figure 4 T2 shine-through effect with DW MR imaging. (a) Transverse fat-suppressed breath-hold singleshot SE echo-planar diffusion image (b 5 × 500 s/mm^2) and (b) corresponding ADC map in a 60-year-old woman with metastatic liver disease. Liver metastasis (arrow), renal cyst, and the gallbladder (∗) show high signal intensity on a. This is clarified on b, where the metastasis shows low diffusivity reflected by the low ADC, while the cyst and the gallbladder show high ADC, not because of restricted water diffusion, but because of the long T2 relaxation time of the fluid (T2 shine-through).[2]

Two out of the five patients with metastases showed a different nature of the hepatic lesions in the same case as some of them showed cystic changes with a relative decrease in the diffusion restriction and elevated ADC value.

One patient had epitheliod-hemangioendothelioma with characteristic target enhancement and capsular retraction with ADC = 0.8×10^{-3} mm^2/s. As EHE is not common histopathological assessment was done to confirm the radiological diagnosis (Fig. 13).

Two patients had cholangiocarcinoma with typical features of delayed centripetal filling in and diffusion restriction with ADC ranging from 0.7 to 1.3×10^{-3} mm^2/s (Fig. 14). Histopathological findings in the two cases confirmed the radiological findings.

MRI with MRCP was superior to CT to diagnose cholangiocarcinoma mainly diagnosis of the exact level of biliary tract involvement and whether it is central or peripheral.

Four patients had focal nodular hyperplasia (FNH) with typical signal intensity and enhancement dynamics as well as no diffusion restriction with ADC ranging from 1.4 to 1.8×10^{-3} mm^2/s (Fig. 15).

In FNH patients both CT and MRI showed the same enhancement dynamics (blush enhancement in HAP with gradual fading till the delayed phase as well as delayed central scar enhancement) yet the MRI was superior to CT in the diagnosis of central scar as it expressed T2 hyperintense signal which differentiated it from fibrolamellar carcinoma that showed T2 hypointense scar. So MRI is of great help to differentiate the scar of FNH from fibrolamellar carcinoma depending on scar and DWI.

Follow up of the four patients with FNH showed no significant changes in size, signal intensity or enhancement pattern of the lesions.
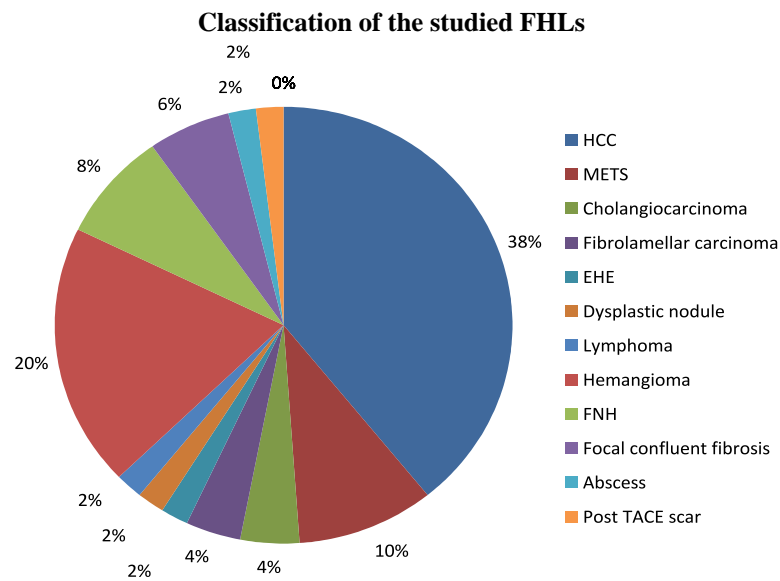
Two patients had fibrolamellar carcinoma on top of the non cirrhotic liver showing the typical signal intensity,


Figure 5 Visual liver lesion characterization with DW MR imaging. This figure gives a simplified approach to lesion characterization by using visual assessment with b of 0 s/mm^2 and a higher b value and ADC maps. A benign fluid-containing lesion shows a strong signal decrease with high ADC, whereas a cellular malignant lesion shows no or minimal signal decrease, with low ADC compared with the surrounding liver parenchyma. A lesion with long T2 can sometimes show a T2 shine through effect (see text for explanations). Black circles are hypointense, white circles are hyperintense.[2]
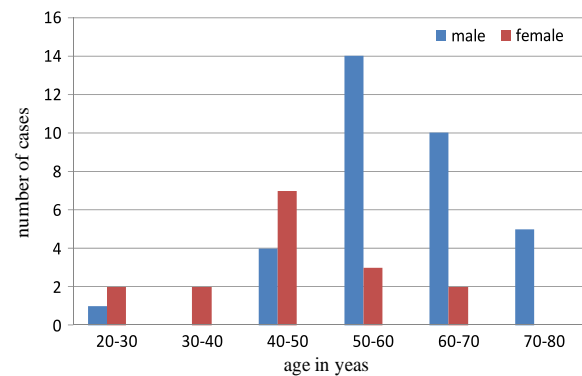
Figure 6 Distribution of the studied group according to their age in relation to the sex.

Classification of the studied FHLs

- HCC
- METS
- Cholangiocarcinoma
- Fibrolamellar carcinoma
- EHE
- Dysplastic nodule
- Lymphoma
- Hemangioma
- FNH
- Focal confluent fibrosis
- Abscess
- Post TACE scar

Figure 7 Distribution of the studied focal hepatic lesions. ∗HCC: hepatocellular carcinoma ∗METS: metastases. ∗EHE: epithelioid-hemangioendothelioma. *FNH: focal nodular hyperplasia ∗TACE: transarterial chemoembolization.
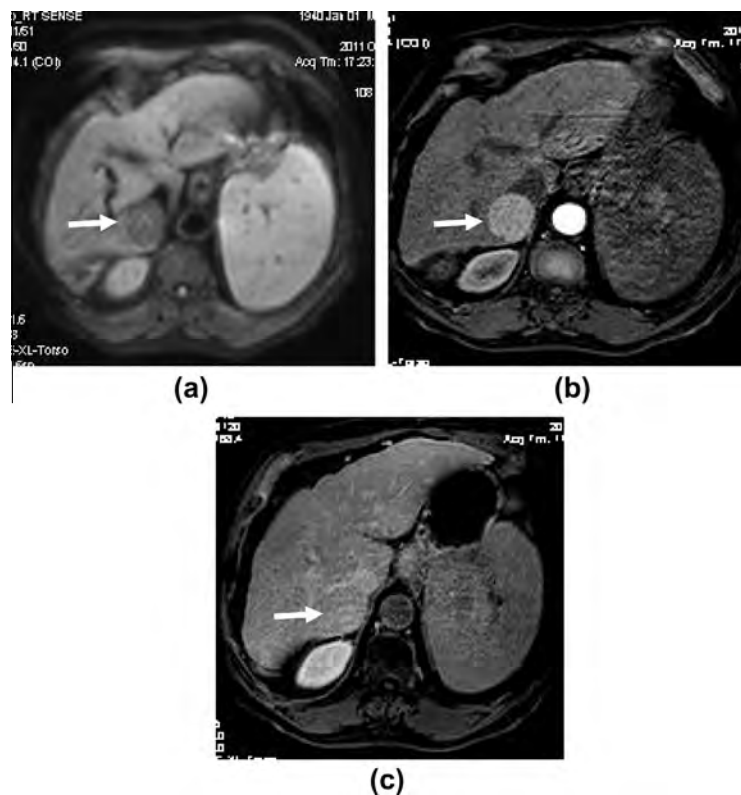

Figure 8 Male patient 71 years with cirrhotic liver showing a well defined dysplastic nodule at segment VI showing no diffusion restriction (arrow in a) enhancement in HAP (arrow in b) and gradual fading in the delayed phase (arrow in c).

with central T2 hypointense scar, enhancement dynamics and diffusion restriction with ADC ranging from 1.1 to 1.2×10^{-3} mm^2/s (Fig. 16).

One patient with lymphoma showed marked diffusion restriction of the hepatic lesions and low ADC = 0.6×10^{-3} mm^2/s.

This patient had multiple hepatic and splenic lesions with marked diffusion restriction of these lesions and very low ADC value. These findings together with enlarged retroperitoneal lymph nodes were enough for the diagnosis of lymphoma and histopathological findings confirmed the radiological diagnosis (Fig. 17).
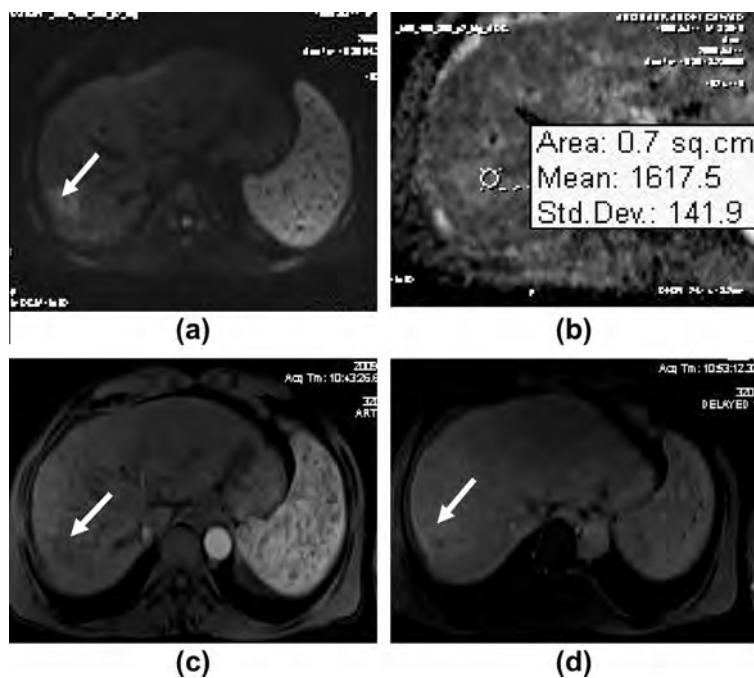
Figure 9 Male patient 53 years with focal confluent fibrosis showing a focal lesion at segment VII hyperintense in DWI (arrow in a) and hyperintense in ADC with its value averaging 1.6×10^3 mm^2/s (b), the lesion showing no definite enhancement in HAP (arrow in c) yet in the delayed phase it took delayed mild enhancement (arrow in d).
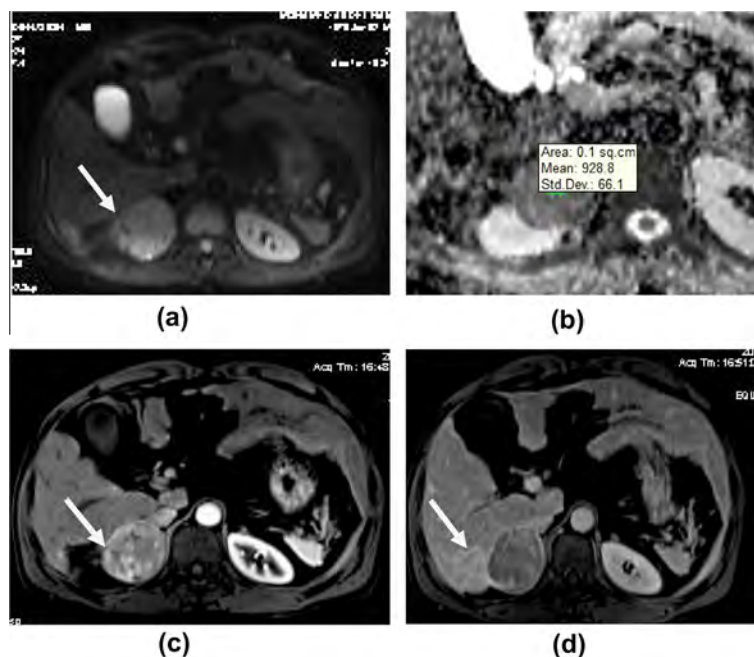

Figure 10 Male patient 40 years showing a classic partially exophytic HCC at segment VI on top of cirrhotic liver showing diffusion restriction in DWI (arrow in a) with ADC value averaging 0.9×10^{-3} mm^2/s (b) washin washout enhancement dynamics with delayed capsular enhancement in the triphasic study (arrows in c and d).

Ten patients had hemangioma with typical signal intensity in a non contrast study as well as enhancement dynamics after contrast injection; they showed no diffusion restriction with characteristic T2 shine through effect with ADC ranging from 1.4 to 2.5×10^{-3} mm^2/s and this was enough for diagnosis of hemangioma with no need for biopsy (Fig. 18).
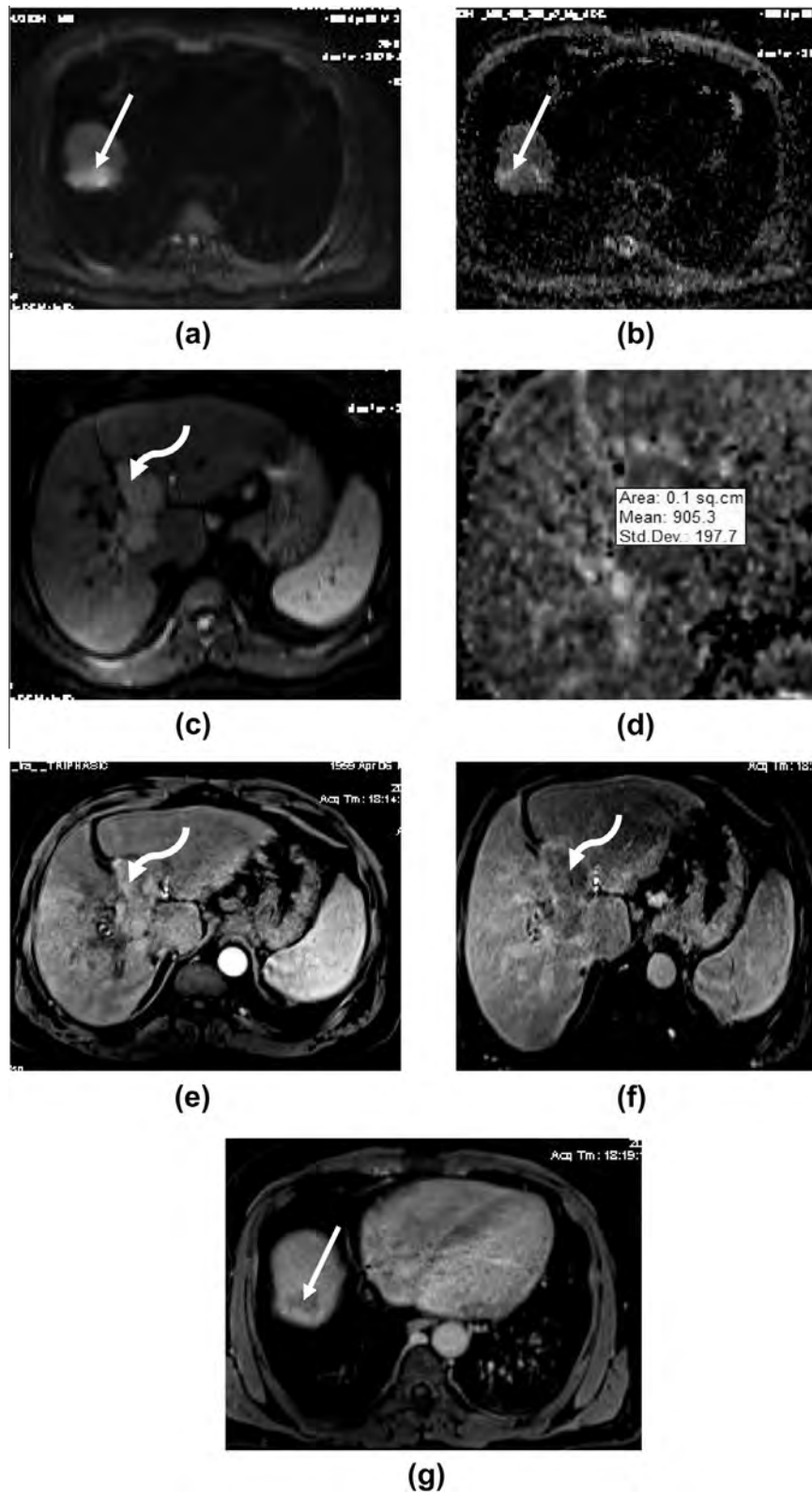
Figure 11 Male patient 51 years showing subcapsular HCC at the hepatic dome with diffusion restriction in DWI (arrow in a) and low ADC (arrow in b), malignant portal vein thrombus is also noted showing diffusion restriction (curved arrow in c) with ADC value averaging 0.9×10^{-3} mm^2/s (d) the malignant thrombus showing the same enhancement dynamics of the main lesion i.e., washin washout pattern (curved arrow in e and f) the main lesion in the delayed phase showing washout with delayed capsular enhancement (arrow in g).
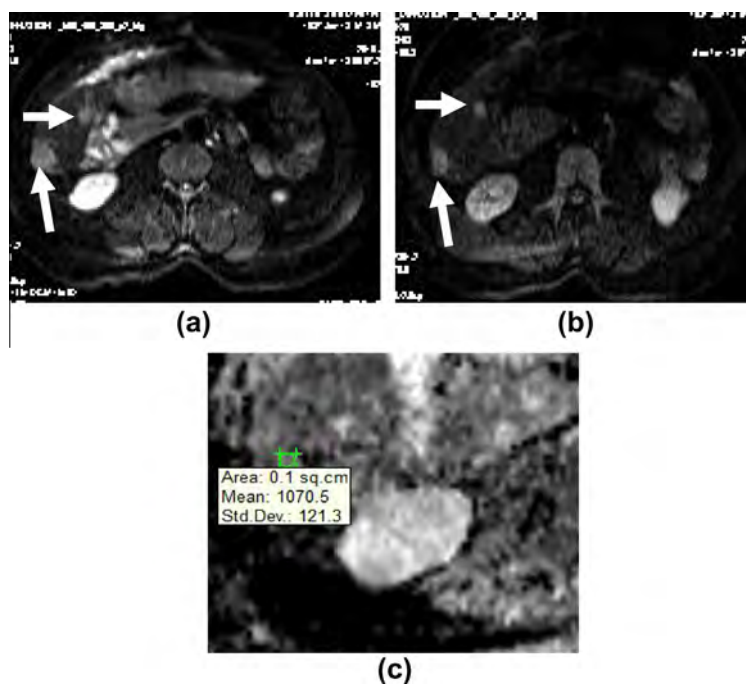
Figure 12 Male patient 78 years with hepatic metastases from colon cancer showing two focal hepatic lesions at segments VI (arrows in a and b) persistent diffusion restriction in high b values ($b = 1000$, (arrows in b). Also note low ADC value averaging 1×10^{-3} mm^2/s.
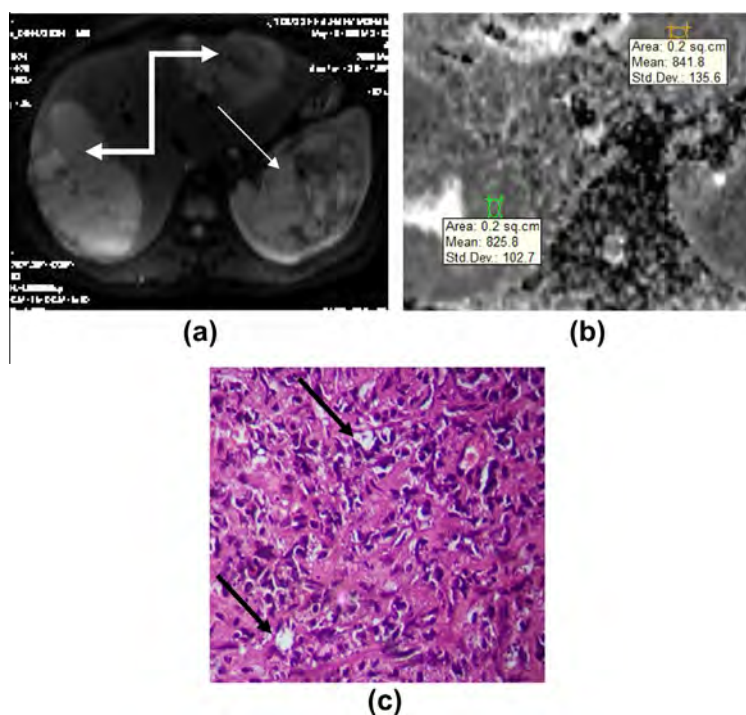
Figure 13 Male patient 49 years with EHE showing diffusion restriction of the hepatic and splenic lesions (arrows in a) with ADC value averaging 0.8×10^{-3} mm^2/s (b) confirmed by histopathological correlation. (c) Epithelioid hemangioendothelioma. Clusters of tumor cells with abundant eosinophilic cytoplasm and hyperchromatic nuclei are seen embedded in a fibrotic stroma. Some of the tumor cells contain cytoplasmic vacuoles representing vascular lumen (arrows). (H&E stain. Original magnification ×100).

Combined two different lesions were found in the same patient, HCC and hemangioma, DWI was of great help with the dynamic study to confirm the diagnosis, it showed T2 shine through the effect of hemangioma and true diffusion restriction of HCC (Fig. 19).

One patient had multiple hepatic abscesses showing marked diffusion restriction with low ADC = 0.8×10^{-3} mm^2/s. In this patient clinical data in correlation with the MRI findings were in favor of the diagnosis of hepatic abscesses which was confirmed by cytological examination of the aspirate from the lesion.

3.1. ADC value

The ADC value of benign lesions ranged from 0.8 to 2.5×10^{-3} mm^2/s while that of the malignant lesions ranged from 0.6 to 1.4×10^{-3} mm^2/s. The low ADC value in benign lesions is attributed to hepatic abscess with increased viscosity which decrease the diffusibility rather than the cellularity and on the other hand the high ADC value in malignant lesions is attributed to cases with hepatic metastases showing cystic changes that relatively increased the ADC value, so from this we found some overlap in ADC value between the benign and malignant lesions however this is not

confusing when the lesion interpretation does not rely only on DWI but is done in conjunction with the other MRI sequences and in correlation with the patient's history.

Statistical analysis of ADC value in different lesions showed the following (Fig. 20).

3.2. Area under curve = 0.947

The cutoff value of ADC for benign lesion is 1.25×10^{-3} mm^2/s, so lesions with ADC less than 1.25×10^{-3} mm^2/s are malignant while lesions with ADC value more than 1.25×10^{-3} mm^2/s are benign with a sensitivity of 90.9% and a specificity of 90.6%.

4. Discussion

In Egypt we are facing the problem of post-hepatitic liver cirrhosis with its complications and radiological dilemmas of different nodular lesions starting from macroregenerative and dysplastic nodules and ending with HCC. Therefore the use of the most accurate and less invasive and less hazardous imaging techniques in diagnosis of these nodular lesions is our goal.
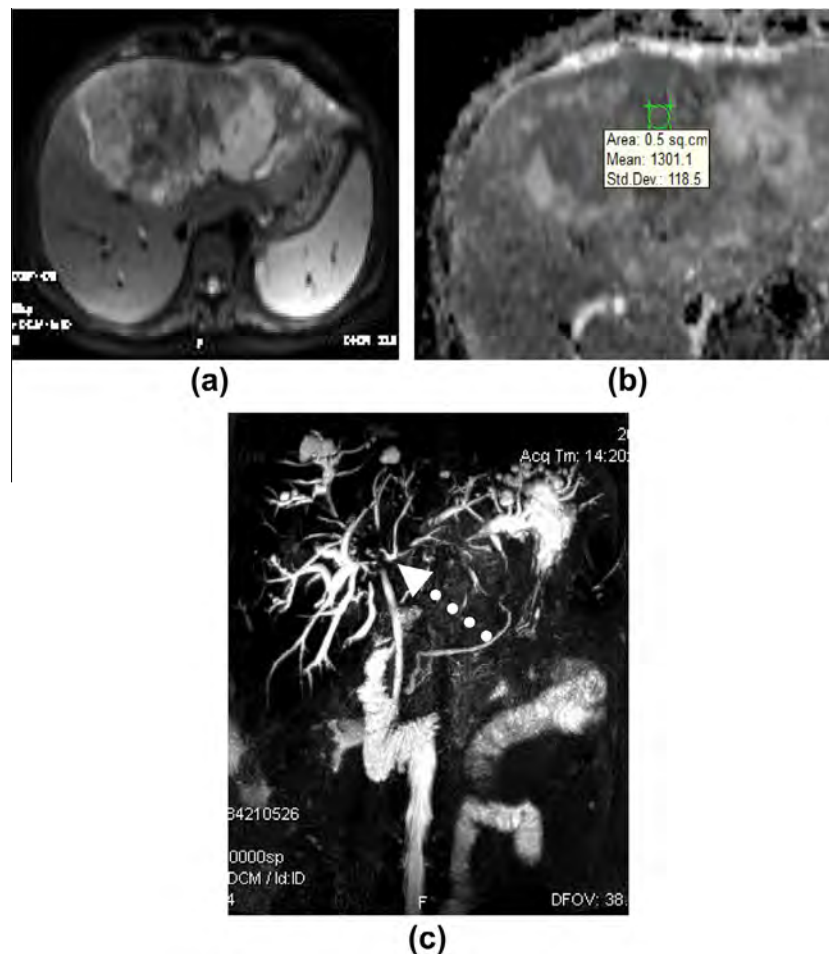

Figure 14 Female patient 41 years with peripheral cholangiocarcinoma showing diffusion restriction (a) with ADC value averaging 1.3×10^{-3} mm^2/s (b) and infiltrating & exerting mass effect upon the biliary radicles in MRCP (dashed arrow in c).
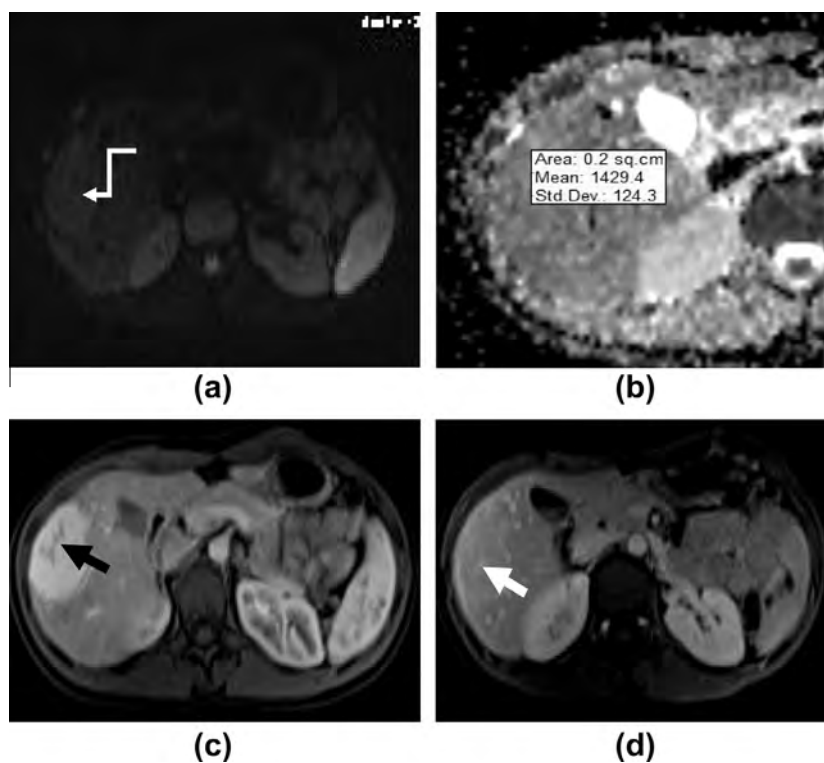
Figure 15 Female patient 34 years with FNH on top of non cirrhotic liver showing no diffusion restriction in DWI (arrow in a) with ADC value averaging 1.4×10^{-3} mm^2/s (b) intense enhancement in HAP (c) and fading in the delayed phase (d) with delayed central scar enhancement (arrow in d).
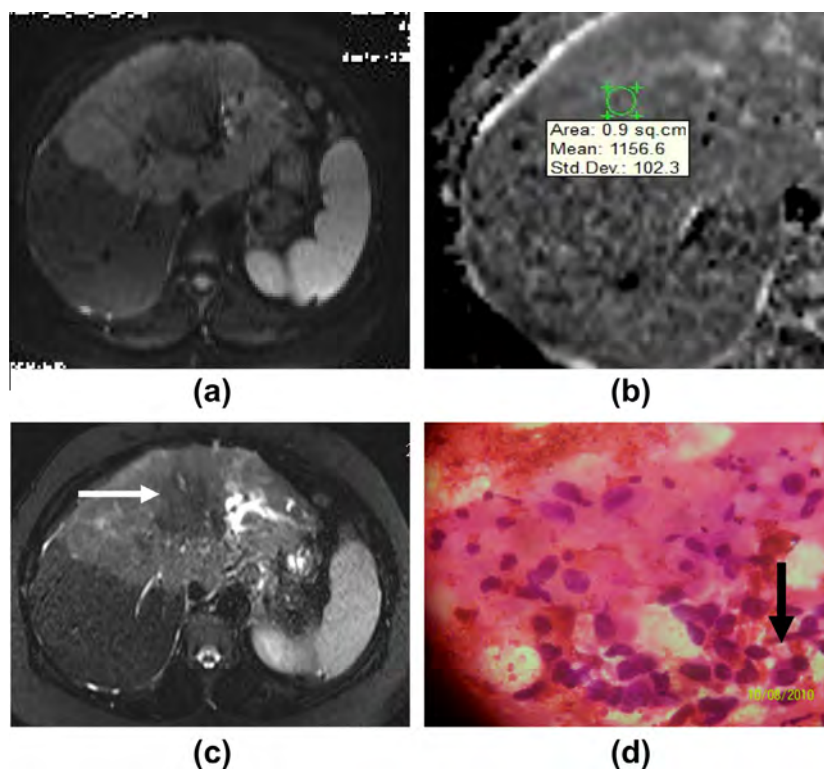
Figure 16 Female patient 50 years with large fibrolamellar carcinoma on top of non cirrhotic liver showing diffusion restriction in DWI (a) with ADC value averaging 1.1×10^{-3} mm^2/s (b) central T2 hypointense scar (arrow in c) and cytological findings confirmed the diagnosis. (d) FNAC of fibrolamellar carcinoma showing tumor cells with abundant eosinophilic cytoplasm embedded in an eosinophilic background and admixed with few spindled fibroblasts (arrow). (H&E stain. Original magnification ×400).
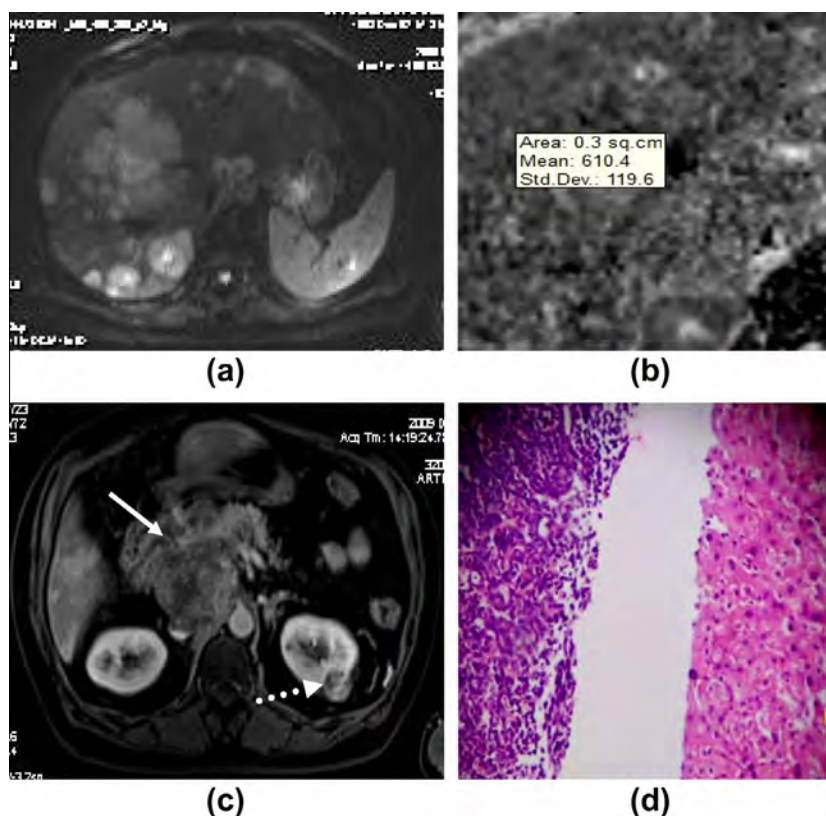
Figure 17 Male patient 56 years with NHL showing multiple lesions infiltrating both lobes of the liver showing diffusion restriction in DWI (a) with low ADC value averaging 0.6×10^{-3} mm^2/s (b), portahepatis and peripancreatic enlarged amalgamated lymph nodes are also noted (arrow in c), also note left renal lesion (dashed arrow in c). Pathologically proved to be NHL (d) Two liver cores from the same patient with NHL, illustrating the nodular pattern of the infiltrate; the liver core on the left side is infiltrated by a neoplastic lymphoid population, while the core on the right shows unremarkable hepatocytes. (H&E stain. Original magnification ×100).

DWI in conjunction with the routine MRI sequences helped us in our cases to differentiate regenerative/dysplastic nodules from early small HCC focus which is of great benefit to the patients in their management.

In addition to the lesions which commonly occur on top of cirrhotic livers there are also other common lesions not associated with cirrhosis such as metastases, hemangioma and FNH that need accurate non-invasive diagnosis for proper management of the patient. With the use of a triphasic CT we can accurately diagnose most of these lesions however the use of MRI with different pulse sequences, triphasic study as well as DWI, which reflect the cellularity of the lesions, and without exposure to radiation helped us to reach the accurate diagnosis.

MRI of the liver is an important tool for the detection and characterization of focal liver lesions. With recent advances in technology, functional MRI methods such as DW is increasingly used in the abdomen with promising results, particularly in the evaluation of focal liver diseases.[9,15,16]

However, although MRI is more superior and less hazardous than CT in the diagnosis of hepatic lesions, it needs a cooperative patient in a relatively longer time of examination when compared with CT and also it is more expensive than CT especially if not covered by health insurance.

DWI may depict and help characterize focal hepatic lesions. A small amount of diffusion weighting with a low b value

(< 200 s/mm^2) nulls the intrahepatic vascular signal intensity, creating the so-called black-blood images and improve depiction of focal liver lesions. Studies have demonstrated the superiority of DWI over T2-weighted MR imaging for depiction of lesions.[9,17] Images with higher b values provide diffusion information that aids in lesion characterization.[9,17] Malignant lesions have lower mean ADC values than benign lesions, with varying degrees of overlap.[9,18,19] In our study we depended upon DWI of both low and high b values in interpretation of the lesion: with low b value, the lesion detectability was high and with the high b value, the lesion characterization was better. This is in association with the quantitative method, i.e., the ADC value helped in differentiating benign from malignant lesions.

In our study, we found an overlap in ADC value between benign and malignant lesions such as in hepatic abscess as it is a benign lesion but with low ADC and in cases of cystic changes of hepatic metastasis with relatively increased ADC value although it is a malignant lesion. This is in agreement with Parikh T DS and Lee VS who found some overlap in ADC value between benign and malignant lesions.[9]

The cutoff value of the benign lesions in our study was 1.25×10^{-3} mm^2/s with a sensitivity of 90.9% and a specificity of 90.6%.

Girometti et al. showed an area under the curve of 0.96, sensitivity of 92%, specificity of 100%, positive predictive
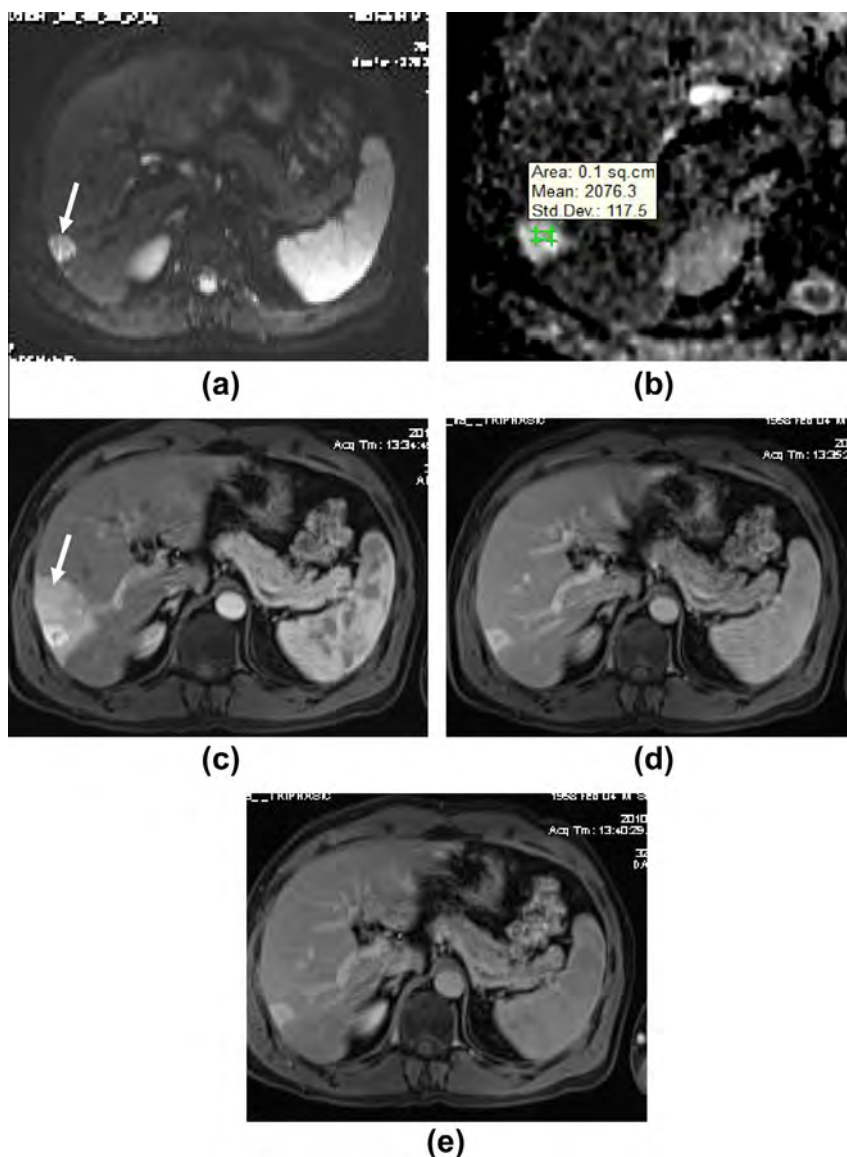
Figure 18 Male patient 52 years with hepatic hemangioma on top of non cirrhotic liver showing high signal intensity in DWI (arrow in a) and high ADC averaging 2×10^{-3} mm^2/s (b), isointense to the aorta in all phases of triphasic study (c–e), wedge shaped area of THID is noted in HAP (arrow in c).

value of 100%, negative predictive value of 99%, and accuracy of 96% using ADC cutoff of 1.31×10^{-3} mm^2/s^2.

DWI is available at most facilities and may be incorporated into conventional protocols. Information from DWI should always be interpreted in conjunction with conventional MR imaging findings.[20,21]

Gourtsoyianni et al.[19] demonstrated higher liver-to-lesion signal intensity ratios with small diffusion gradients for HCC and metastatic lesions. Similarly our results demonstrated the value of DWI in detection of focal liver lesions including HCC and metastases, as MRI in HCC patients showed the same CT findings but with superior lesion-to-liver contrast with no exposure to radiation and confidently diagnosed the HCC by using different pulse sequences in addition to DWI.

In one of our cases the patient had both HCC and hemangioma, both lesions could be differentiated confidently by the DWI together with other MRI sequences and triphasic study, and this differentiation is important to select patients that can undergo liver biopsy.

Results of a study by Low et al.[20] have shown increased detection of metastatic lesions with a combination of DWI and precontrast T1- and T2-weighted imaging. This is in concordance with our results that highlighted the complementary role of DWI with routine MRI in diagnosis and characterization of metastatic lesions.

Low and Gurney[20] published a study recently that demonstrated the additional detection of tumor foci with DWI compared with that of conventional sequences (pre- and post contrast imaging), the potential benefit of DWI in association or comparison with conventional gadolinium-enhanced liver MRI remains to be investigated. Our study showed the complementary role of diffusion in the detection of primary and metastatic lesions of the liver.
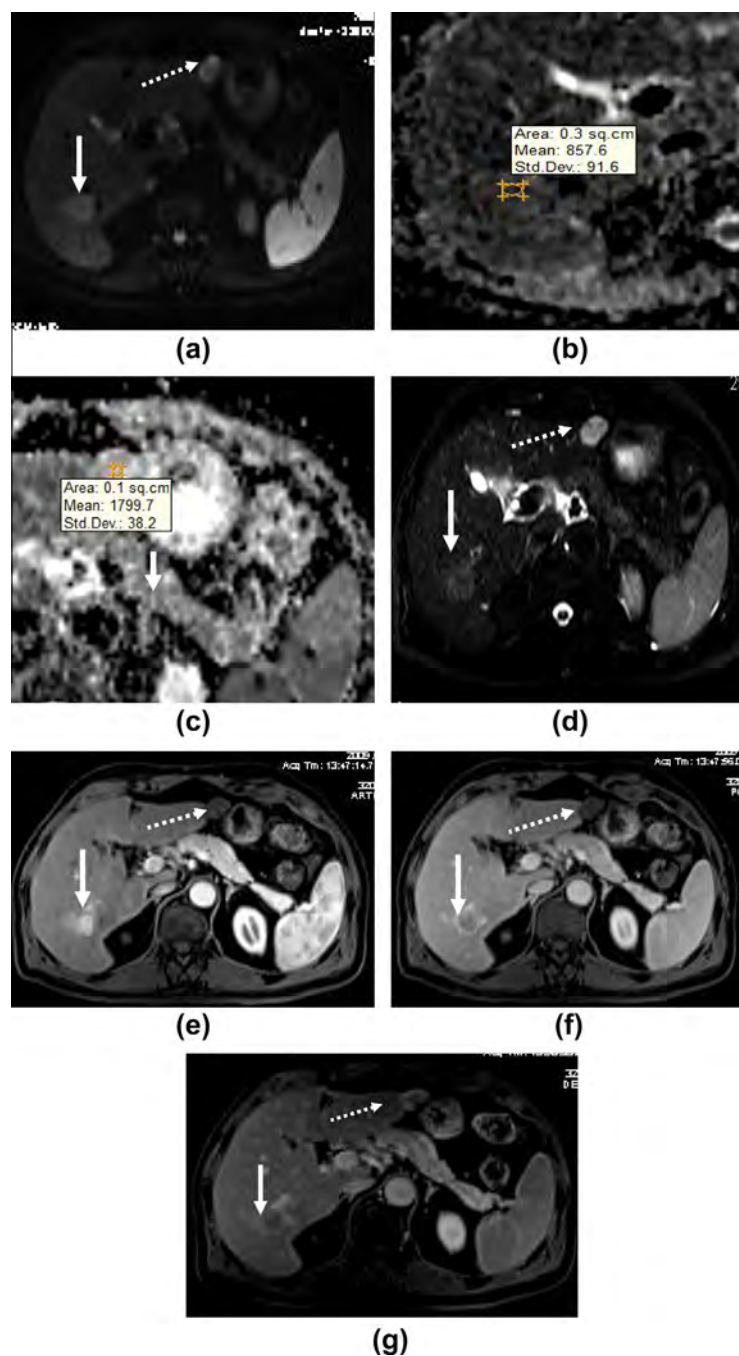
Figure 19 Male patient 60 years with HCC at the right lobe showing diffusion restriction, hyperintese in DWI (arrow in a) with ADC value averaging 0.85×10^{-3} mm^2/s (b) and hemangioma at the left lobe showing T2 shine through effect in DWI (dashed arrow in a) with ADC value averaging 1.8×10^{-3} mm^2/s (c), the hemangioma showing a light bulb appearance in long TE in T2WI (dashed arrow in d) while HCC showing less T2 hyperintense signal (arrow in d), the hemangioma showing peripheral enhancement in HAP (dashed arrow in e) with gradual filling in PVP and delayed phase (dashed arrow in f and g respectively) while HCC showing washin washout enhancement dynamics (arrow in e–g).

DWI enabled us to discriminate between bland and neo-plastic portal vein thrombus in a case of HCC, as the thrombus showed similar signal intensity as the primary HCC when qualitative analysis was performed. This was previously mentioned by Parikh et al.[9] and by Onofrio et al.[22].

5. Conclusion

DWI is an important complementary sequence with the routine MRI of the liver that helps in lesion quantification and characterization in a hope to reach final confident diagnosis and in order to reduce the rate of biopsy.
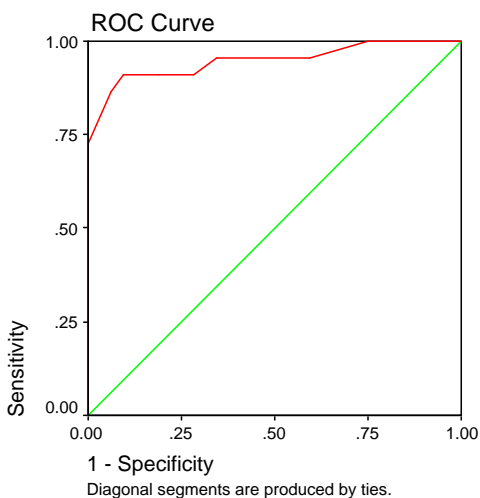
Figure 20   ROC curve of ADC of benign lesions.

The use of a quantitative method using ADC value with a cutoff point of 1.25×10^{-3} mm^2/s is helpful in differentiating benign from malignant lesions.

Although the MRI is a safe technique without exposure to radiation it has some disadvantages as the examination takes longer time than in CT and it is also more expensive than CT especially in our country with limited resources.

Therefore, MRI and DWI should be used in selected lesions where their use would add benefit to the patient.

Conflict of interest

None declared.

References

1. Qayyum A. Diffusion-weighted imaging in the abdomen and pelvis: concepts and applications. *Radiographics* 2009;**29**:1797–810.
2. Bachir Taouli DMK. Diffusion-weighted MR Imaging of the liver. *Radiology* 2010;**254**:47–66.
3. Furukawa MKK, Kamada H, Miyasaka K. MRI in seven cases of tacrolimus (FK-506) encephalopathy: utility of FLAIR and diffusion-weighted imaging. *Neuroradiology* 2001;**43**:615–21.
4. Berman JI. Diffusion tensor imaging-guided tracking of fibers of the pyramidal tract combined with intraoperative cortical stimulation mapping in patients with gliomas. *J Neurosurg* 2004;**101**:66–72.
5. Takeuchi MNH, Mori K, Sakama M. Magnetic resonance imaging and proton MR spectroscopy of the brain in a patient with carbohydrate deficient glycoprotein syndrome type I. *J Magn Reson Imaging* 2003;**17**:722–5.
6. DTB M. Diffuse liver disease:strategies for hepatic CT and MR imaging. *Radiographics* 2009;**29**:1591–614.
7. Koh DM, Collins DJ. Diffusion-weighted MRI in the body: applications and challenges in oncology. *AJR* 2007;**188**:1622–35.
8. Patterson DMCD. Technology insight: water diffusion MRI—a potential new biomarker of response to cancer therapy. *Nat Clin Pract Oncol* 2008;**5**:220–33.
9. Parikh T, Lu DS, et al. Focal liver lesion detection and characterization with diffusion-weighted MR imaging: comparison with standard breath-hold T2-weighted imaging. *Radiology* 2008;**246**:812–22.
10. Hussain DBJ HW et al. Can a single-shot black-blood T2-weighted spin-echo echo planar imaging sequence with sensitivity encoding replace the respiratory-triggered turbo spin-echo sequence for the liver? An optimization and a feasibility study. *J Magn Reson Imaging* 2005;**21**:219–29.
11. Van den Bos ICKG, Wielopolski PA. Liver imaging at 30 T:diffusion-induced black-blood echo-planar imaging with large anatomic volumetric coverage as an alternative for specific absorption rate-intensive echo-train spin-echo sequences: feasibility study. *Radiology* 2008;**284**:264–71.
12. Taouli BDJ, Fan B, Menu Y. Evaluation of liver diffusion isotropy and characterization of focal hepatic lesions with two single-shot echoplanar MR imaging sequences: prospective study in 66 patients. *Radiology* 2003;**226**:71–8.
13. Taouli BLM et al. Diffusion-weighted MRI for quantification of liver fibrosis: preliminary experience. *AJR* 2007;**189**:799–806.
14. Taouli B, Qayyum A, Coakley FV, Vilgrain V. Chronic hepatitis: role of diffusion-weighted imaging and diffusion tensor imaging for the diagnosis of liver fibrosis and inflammation. *J Magn Reson Imaging* 2008;**28**:89–95.
15. HC BT. Diffusion and perfusion imaging of the liver. *Europ J Radiol* 2010;**76**:348–58.
16. Xi-Jie Sun, Xian-Yue Quan, Fan-Heng Huang, Yi-Kai Xu. Quantitative evaluation of diffusion-weighted magnetic resonance imaging of focal hepatic lesions. *World J Gastroenterol* 2005;**11**:6535–7.
17. Bruegel MGJWS et al. Diagnosis of hepatic metastasis: comparison of respiration-triggered diffusion-weighted echo-planar MRI and five T2-weighted turbo spin-echo sequences. *AJR* 2008;**191**:1421–9.
18. Bruegel M, GJ HK, et al. Characterization of focal liver lesions by ADC measurements using a respiratory triggered diffusion-weighted single-shot echo-planar MR imaging technique. *Eur Radiol* 2008;**18**:477–85.
19. Gourtsoyianni S, Papanikolaou N, Yarmenities S, Maris T, Karantanas A, Gourtsoyiannis N. Respiratory gated diffusion-weighted imaging of the liver: value of apparent diffusion coefficient measurements in the differentiation between most commonly en-countered benign and malignant focal liver lesions. *Eur Radiol* 2008;**18**:486–92.
20. Low RN, Gurney J. Diffusion-weighted MRI (DWI) in the oncology patient: value of breathhold DWI compared to unenhanced and gadolinium-enhanced MRI. *J Magn Reson Imaging* 2007;**25**:848–58.
21. Daniella B, Parente RMP, Antonio Eiras-Araujo, Jaime A, Oliveira Neto, Edson Marchiori, et al. MR imaging of hypervascular lesions in the cirrhotic liver: a diagnostic dilemma. *RadioGraphics* 2012;**32**:767–87.
22. Onofrio A, Catalano GC, Hahn Peter F, Sahani Dushyant V. Differentiation of malignant thrombus from bland thrombus of the portal vein in patients with hepatocellular carcinoma: application of diffusion-weighted MR imaging. *Radiology* 2010;**254**:154–62.